NANO LETTERS

Letter

pubs.acs.org/NanoLett

Electrically Tunable Damping of Plasmonic Resonances with Graphene

Naresh K. Emani,[†,§] Ting-Fung Chung,[‡,§] Xingjie Ni,[†,§] Alexander V. Kildishev,[†,§] Yong P. Chen,[‡,†,§] and Alexandra Boltasseva*[,†,§,∥]

[†]School of Electrical and Computer Engineering, [‡]Department of Physics, and [§]Birck Nanotechnology Center, Purdue University, West Lafayette, Indiana 47907, United States

[∥]DTU Fotonik, Department of Photonics Engineering, Technical University of Denmark, Lyngby DK-2800, Denmark

Supporting Information

ABSTRACT: Dynamic switching of a plasmonic resonance may find numerous applications in subwavelength optoelectronics, spectroscopy, and sensing. Graphene shows a highly tunable carrier concentration under electrostatic gating, and this could provide an effective route to achieving electrical control of the plasmonic resonance. In this Letter, we demonstrate electrical control of a plasmonic resonance at infrared frequencies using large-area graphene. Plasmonic structures fabricated on graphene enhance the interaction of the incident optical field with the graphene sheet, and the impact of graphene is much stronger at mid-infrared wavelengths. Full-wave simulations, where graphene is modeled as a 1 nm thick effective medium, show excellent agreement with experimental results.

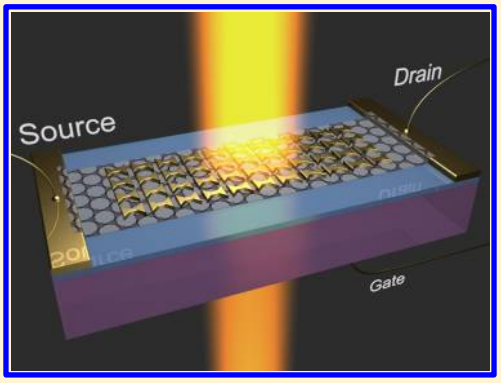

KEYWORDS: *Graphene, plasmonics, tunable resonances, interband losses*

Plasmonics offers an exciting route to subwavelength optoelectronics by confining the optical fields below the diffraction limit.[1,2] This is achieved by employing metal nanostructures that are resonant at a particular optical wavelength. The resonance wavelength of the nanostructure can be tuned by varying the size, shape, and material properties of the structure. However, in some applications like integrated modulators, switches, and sensors, it is desirable to have the ability to dynamically tune the resonance wavelength, preferably by applying an electrical bias. Indeed, electrical control of resonances has been demonstrated at terahertz frequencies.[3−5] Similar dynamic switching of plasmonic resonances at optical wavelengths could open up many exciting possibilities.

In this Letter, we use graphene to electrically tune a plasmonic resonance. Graphene, which is composed of a hexagonal lattice of sp^2 carbon atoms arranged in a single sheet and exhibits extraordinary electrical and optical properties,[6,7] was previously proposed as a novel platform for integrated optoelectronics and transformation optics.[8,9] Graphene also shows some remarkable effects when the material interacts with split-ring resonator-based metamaterials,[10] nanoantennas,[11−12] localized surface plasmons,[13] and in on-chip optical modulators.[14] Several recent studies have demonstrated the excitation of terahertz plasmons in graphene.[15−17] In the visible and near-IR frequencies, however, the interband loss becomes large and makes graphene unattractive as a plasmonic material.[18,19] Alternatively, the optical loss in graphene could instead be used as an advantage in order to vary the loss of a plasmonic resonance. Here we show that it is indeed possible to electrically control the width of the plasmonic resonance using graphene. Very recently, a closely related approach was applied to electrically control plasmonic resonances in gold nanorods.[20]

Graphene exhibits a unique linear dispersion relation as shown in Figure 1a. The carrier density (n_{2D}) in a graphene sheet can be electrically controlled by an applied gate voltage, thereby leading to a voltage-controlled Fermi energy given by $E_F = \hbar v_F(\pi n_{2D})^{1/2}$, where $\hbar$ is the reduced Planck constant and v_F is the Fermi velocity of electrons. The controllable changes in the carrier density modifies the dielectric function of graphene, which can be straightforwardly obtained from its optical conductivity $\sigma(\omega)$ as $\varepsilon_r(\omega) = i\sigma(\omega)/(\omega\varepsilon_0 t_g)$.[9]

Here $\sigma(\omega)$ is calculated within the local random phase approximation (RPA)[8,21] as

$$\sigma(\omega) = \frac{2e^2\omega_T}{\pi\hbar}\frac{i}{\omega + i\tau^{-1}}\log\left[2\cosh\left(\frac{\omega_F}{2\omega_T}\right)\right] + \frac{e^2}{4\hbar}\left[H\left(\frac{\omega}{2}\right) + i\frac{2\omega}{\pi}\int_0^\infty \frac{H\left(\frac{\omega'}{2}\right) - H\left(\frac{\omega}{2}\right)}{\omega^2 - \omega'^2}d\omega'\right] \quad (1)$$

Received: June 21, 2012
Revised: August 27, 2012
Published: September 5, 2012

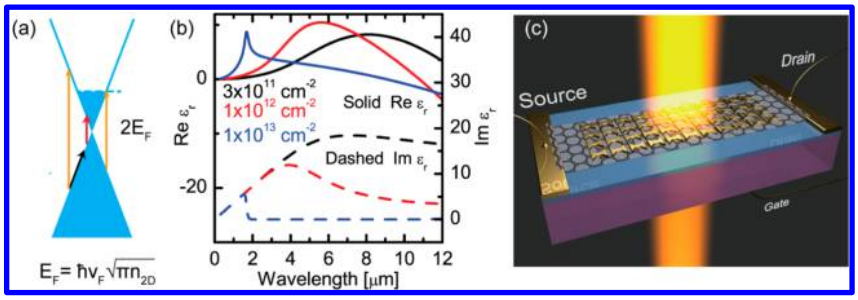

Figure 1. (a) The optical response of graphene is controlled by e-h pair excitations. Photons with energies above $2E_F$ will be absorbed due to transitions into the unoccupied states above the Fermi level; (b) calculated dielectric functions for carrier densities of 3×10^{11}, 1×10^{12}, 1×10^{13} cm^{-2} show a tunable interband threshold. Changes in the imaginary part (dashed lines) of permittivity are accompanied by corresponding changes in the real part (solid lines). The calculations were performed with $\tau = 1 \times 10^{-13}$ s, $T = 300$ K and $t_g = 1$ nm; (c) schematic illustration of the experimental structure for voltage-controlled optical transmission measurements.

where $H(\omega) = \sinh(\omega/\omega_T)/[\cosh(\omega_F/\omega_T) + \cosh(\omega/\omega_T)]$, $\omega_F = E_F/\hbar$, $\omega_T = k_BT/\hbar$, ω is the frequency of incident light, t_g is the graphene thickness, e is the charge of an electron, τ is the Drude relaxation rate, T is the temperature, and k_B is the Boltzmann constant. The first term in eq 1 describes the free-carrier (intraband) response of graphene. The second term captures the response from interband transitions, which exhibit a steplike behavior at 0 K. The tunable Fermi energy leads to a gate-tunable interband threshold wherein an incident photon can generate an electron−hole (e-h) pair only if its energy is higher than $2E_F$. For photons of lower energy there will not be any interband losses at 0 K. The predicted optical conductivity is consistent with experimental measurements.[22−24] At higher temperatures, the interband threshold is broadened but shows qualitatively similar behavior.

In our numerical calculations we have modeled graphene as an effective medium of thickness $t_g = 1$ nm (see Supporting Information Figure S1). The calculated effective dielectric functions at three different carrier concentrations are shown in Figure 1b. For realistic sheet carrier densities in the range 10^{11}−10^{13} cm^{-2}, the interband threshold can be continuously tuned up to near-IR frequencies. When bowtie antennas exhibiting a strong resonance in the IR wavelength range[25] are fabricated on top of a graphene sheet, their optical properties will be significantly influenced by the applied gate voltage. The resonance is accompanied by a local field enhancement that causes enhanced interaction with the graphene sheet. Hence, if the plasmonic resonance frequency is above the graphene interband threshold, then the resonance decays by direct emission of e-h pairs.

Figure 1c shows the schematic of the experimental setup for demonstrating plasmonic resonance tuning. A gate voltage (V_G) is applied through the silicon back-gate. The resistance between the source and drain terminals (R_{SD}) is measured to monitor carrier concentration in graphene sheet. The source−drain contacts were deposited by e-beam evaporation of 10 nm Ti/60 nm Au strips on a lightly doped Si substrate with a previously grown, 100 nm layer of dry thermal oxide. A large-area graphene sheet, which was initially grown on 25 μm copper foil by atmospheric pressure chemical vapor deposition (CVD),[26] was transferred onto the sample substrate while ensuring good electrical connections with both the source and the drain contacts. Next, bowtie structures were fabricated by electron beam lithography, metallization (2 nm Ti and 30 nm Au), and subsequent lift-off processes.

Typical modulation of carrier concentration in graphene with gate voltage is shown in Figure 2a. We define $\Delta V = V_G - V_{DP}$, where V_G is the gate voltage applied and V_{DP} is the gate voltage

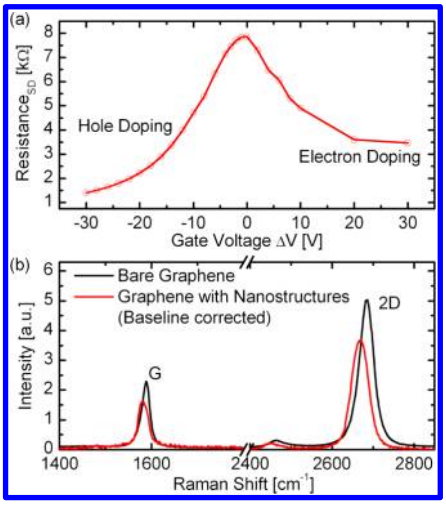

Figure 2. (a) Typical plot of carrier concentration dependence on gate voltage indicating a good modulation of carrier concentration. We also observed a very small variation of resistance during optical measurements, which can be attributed to electrochemical redox reactions of adsorbates on graphene;[27] (b) Raman spectroscopy of graphene with and without metal nanostructures shows electron doping caused by the metal.[28,29] The intensity of the D peak is small, indicating the high quality of the graphene. Spectra were averaged from measurements at three different locations on the sample.

for which graphene exhibits a peak in source−drain resistance (R_{SD}) referred to as Dirac point. Since the resonant structures are in contact with the graphene, they could have an impact on the electronic properties of the graphene. To investigate possible effects from the metal nanostructures, we performed Raman spectroscopy on bare graphene as well as on graphene with metal nanostructures. We observed changes in the graphene carrier concentration caused by additional electron doping due to the metal (see Figure 2b). At the same time, the electrical characteristics remained qualitatively similar to those of bare graphene except for a shift in the Dirac point.

To investigate the impact of graphene on metal nanostructures at different resonant frequencies, we fabricated bowtie antennas of different dimensions as shown in Figure 3a. Bowties 1−3 were fabricated on the same graphene device, and bowtie 4 was fabricated on a different device. A scanning electron micrograph of a fabricated sample with plasmonic structures on top of the graphene sheet is shown in Figure 3c. It is clearly seen that the CVD graphene is mostly uniform, although some folds and domain discontinuities can be observed. A Fourier transform

dx.doi.org/10.1021/nl302322t | Nano Lett. 2012, 12, 5202−5206

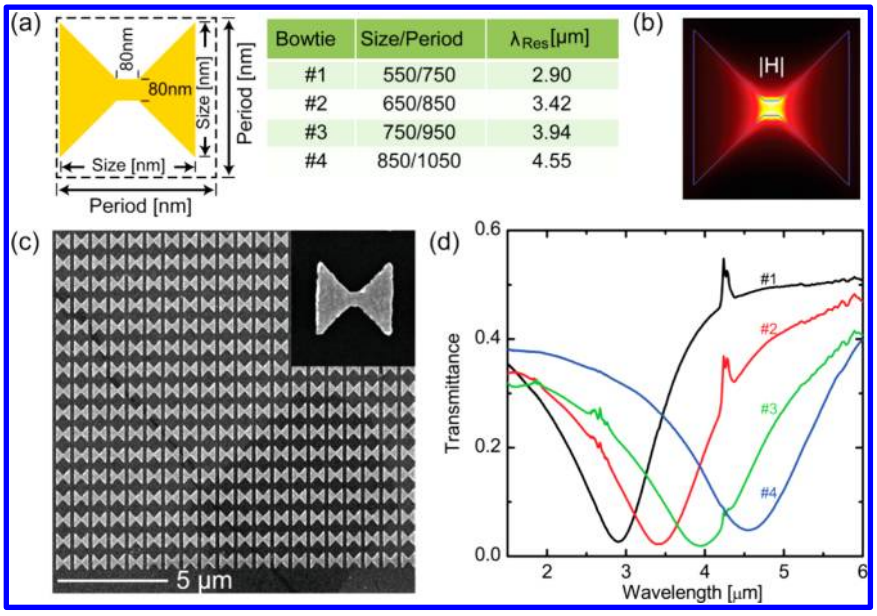

Figure 3. (a) Geometry, dimensions, and resonant wavelengths of fabricated bowtie antennas on graphene. (b) Calculated local magnetic field enhancement at the center of bowtie at resonant wavelength. The bowtie plasmonic resonance is thoroughly discussed by Grosjean et al.[25] (c) Scanning electron micrograph of fabricated bowtie antennas on top of a graphene sheet. (d) Measured optical transmission spectra for bowtie antennas with different periodicities fabricated on graphene.

infrared (FTIR) spectrometer with a microscope was used to optically characterize the plasmonic resonance behavior. All the optical measurements were performed in ambient air at room temperature. The experimentally measured optical transmission spectra of the resonant structures on top of the graphene are shown in Figure 3d. We observe a strong resonance that exhibits a red shift in resonant wavelength with increasing dimensions.

To gain further insight into the experimentally obtained spectra, we performed full-wave numerical simulations using 3D spatial harmonic analysis (SHA).[30] The sample was modeled with four layers: silicon, silicon dioxide, graphene, and gold bowtie antennas with corresponding material properties and geometries taken from experiments. We treated graphene as an effective medium with a thickness of 1 nm, and we calculated its dielectric function using the optical conductivity of graphene (eq 1). To investigate the impact of gate voltage, we used the carrier concentration of the graphene sheet as a fitting parameter in our numerical simulations.

The carrier concentration of graphene can be realistically tuned between 1×10^{12} and 3×10^{13} cm^{-2}, and hence E_F can be varied in the range of 0.12−0.64 eV. Therefore, we can expect a significant impact from the gate voltage on the resonances at IR wavelengths. To investigate this dependence we compared the optical transmission spectra from three structures (Bowtie 1−3) fabricated on the same device. We found that the effect of the gate voltage on the resonance increases as the resonant frequency shifts further into IR as shown in Figure 4. We observed that the change for graphene with bowtie antennas was much higher than the approximately 1% change in a bare graphene device (shown in Supporting Information Figure S2). This is consistent with the results reported in the published literature,[15,22] confirming that plasmonic structures do indeed enhance the interaction of light with graphene.

The optical transmission spectrum for a resonance at 4.5 μm is shown in Figure 5a where we see an observable variation of transmittance with gate voltage. At the Dirac point ($\Delta V = V_G - V_{DP} = 0$), the interband transitions are allowed at all frequencies, leading to a broader resonance. However, with increasing carrier concentration ($\Delta V < 0$) some of the interband transitions are forbidden, leading

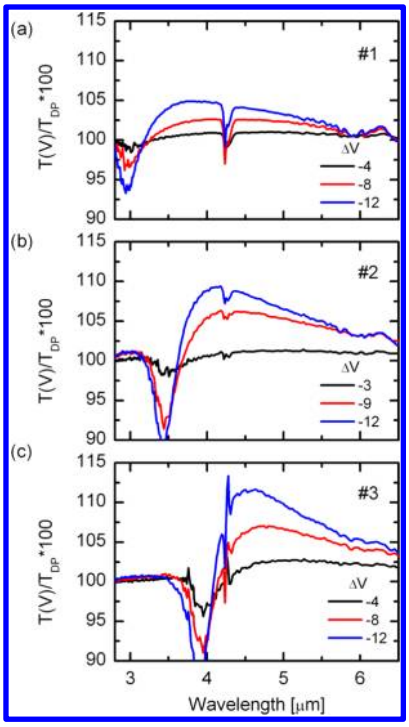

Figure 4. The measured transmittance at a particular gate bias (in volts) normalized by the transmittance measured at the Dirac point. The carrier concentration in graphene increases as ΔV moves away from zero and leads to a stronger impact on resonance. We observe stronger damping of the plasmonic resonance at mid-infrared wavelengths. Data for Bowties #1, #2 and #3 is shown in panels (a), (b) and (c) respectively.

to narrower line width. The asymmetric influence of graphene on the line shape reflects the changes in the dielectric function plotted in Figure 1b. The full-wave numerical electromagnetic simulations show remarkable agreement with the experimental results using only the carrier concentration in graphene as a fitting parameter. We observe up to 210 nm decrease in resonance line

dx.doi.org/10.1021/nl302322t | Nano Lett. 2012, 12, 5202−5206

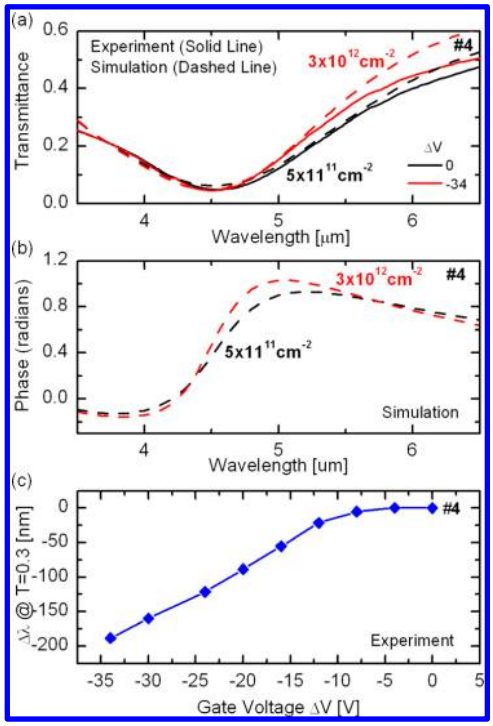

Figure 5. (a) Experimentally observed (solid lines) damping of a plasmonic resonance due to an applied gate voltage. A higher carrier concentration leads to blocking of some interband transitions, and hence leads to a narrower resonance. Full-wave simulations (dashed lines) performed with graphene carrier concentration as a fitting parameter produce an excellent match with the experimental results. (b) Simulated phase delay of *E*-field along the axis of the bowtie. Changes in carrier concentration lead to a simultaneous change in transmission as well as phase since both real and imaginary parts of permittivity of graphene are tuned by electric bias. (c) The narrowing of the width of the resonance with gate bias shows the precise electrical control of the resonance.

width with applied bias. Further, in addition to the damping that is expected from the absorption due to graphene, we also see a small blue shift in the resonance. This is not surprising as the changes in the real part of permittivity lead to change in the resonant wavelength.

On the basis of simulations it has been suggested previously that adding graphene on top of resonant structures could significantly change the transmittance when the resonant electric field is parallel to the graphene sheet.[31] In contrast, we observe a strong asymmetric influence of graphene on resonance line shape in our bowtie antennas where the electric field is parallel to the graphene. We believe that a greater degree of control of plasmonic resonance can be achieved by further understanding of interaction of graphene with metal nanostructures.

In summary, we show that graphene can be used to electrically control the damping of plasmonic resonances in the mid-infrared part of the spectrum. The framework developed in this work will be useful to further explore designs to achieve stronger damping and tuning of plasmonic resonances

■ ASSOCIATED CONTENT

Supporting Information

Additional information on choice of effective thickness of graphene in numerical simulations and optical transmission measurements of device without bowtie antennas are included. This material is available free of charge via the Internet at http://pubs.acs.org.

■ AUTHOR INFORMATION

Corresponding Author

*E-mail: aeb@purdue.edu.

Notes

The authors declare no competing financial interest.

■ ACKNOWLEDGMENTS

We thank Professor Vladimir M. Shalaev for useful discussions. This work was supported in part by ARO MURI Grant 56154-PH-MUR (W911NF-09-1-0539) and ARO Grant 57566-PHRIP (W911NF-10-1-0380). A.V.K. was supported in part by AFRL Materials and Manufacturing Directorate Applied Metamaterials Program. The graphene synthesis and characterization were supported in part by NSF (DMR 0847638) and DTRA (HDTRA1-09-1-0047).

■ REFERENCES

(1) Lal, S.; Link, S.; Halas, N. J. *Nat. Photonics* **2007**, *1* (11), 641−648.
(2) Brongersma, M. L.; Shalaev, V. M. *Science* **2010**, *328* (5977), 440−441.
(3) Chen, H. T.; Padilla, W. J.; Zide, J. M. O.; Gossard, A. C.; Taylor, A. J.; Averitt, R. D. *Nature* **2006**, *444* (7119), 597−600.
(4) Padilla, W. J.; Taylor, A. J.; Highstrete, C.; Lee, M.; Averitt, R. D. *Phys. Rev. Lett.* **2006**, *96* (10), 107401.
(5) Driscoll, T.; Kim, H. T.; Chae, B. G.; Kim, B. J.; Lee, Y. W.; Jokerst, N. M.; Palit, S.; Smith, D. R.; Di Ventra, M.; Basov, D. N. *Science* **2009**, *325* (5947), 1518−1521.
(6) Geim, A. K.; Novoselov, K. S. *Nat. Mater.* **2007**, *6* (3), 183−191.
(7) Bonaccorso, F.; Sun, Z.; Hasan, T.; Ferrari, A. *Nat. Photonics* **2010**, *4* (9), 611−622.
(8) Koppens, F. H. L.; Chang, D. E.; García de Abajo, F. J. *Nano Lett.* **2011**, *11* (8), 3370−3377.
(9) Vakil, A.; Engheta, N. *Science* **2011**, *332* (6035), 1291.
(10) Papasimakis, N.; Luo, Z.; Shen, Z. X.; De Angelis, F.; Di Fabrizio, E.; Nikolaenko, A. E.; Zheludev, N. I. *Opt. Express* **2010**, *18* (8), 8353−8359.
(11) Fang, Z.; Liu, Z.; Wang, Y.; Ajayan, P. M.; Nordlander, P.; Halas, N. J. *Nano Lett.* **2012**, *12* (7), 3808−3813.
(12) Echtermeyer, T.; Britnell, L.; Jasnos, P.; Lombardo, A.; Gorbachev, R.; Grigorenko, A.; Geim, A.; Ferrari, A.; Novoselov, K. *Nat. Commun.* **2011**, *2*, 458.
(13) Niu, J.; Jun Shin, Y.; Lee, Y.; Ahn, J. H.; Yang, H. *Appl. Phys. Lett.* **2012**, *100* (6), 061116−061116−4.
(14) Liu, M.; Yin, X.; Ulin-Avila, E.; Geng, B.; Zentgraf, T.; Ju, L.; Wang, F.; Zhang, X. *Nature* **2011**, *474* (7349), 64−67.
(15) Ju, L.; Geng, B. S.; Horng, J.; Girit, C.; Martin, M.; Hao, Z.; Bechtel, H. A.; Liang, X. G.; Zettl, A.; Shen, Y. R.; Wang, F. *Nat. Nanotechnol.* **2011**, *6* (10), 630−634.
(16) Fei, Z.; Rodin, A. S.; Andreev, G. O.; Bao, W.; McLeod, A. S.; Wagner, M.; Zhang, L. M.; Zhao, Z.; Thiemens, M.; Dominguez, G.; Fogler, M. M.; Neto, A. H. C.; Lau, C. N.; Keilmann, F.; Basov, D. N. *Nature* **2012**, *487* (7405), 82−85.
(17) Chen, J.; Badioli, M.; Alonso-Gonzalez, P.; Thongrattanasiri, S.; Huth, F.; Osmond, J.; Spasenovic, M.; Centeno, A.; Pesquera, A.; Godignon, P.; Zurutuza Elorza, A.; Camara, N.; Javier Garcia de Abajo, F.; Hillenbrand, R.; Koppens, F. H. L. *Nature* **2012**, *487* (7405), 77−81.
(18) Jablan, M.; Buljan, H.; Soljačić, M. *Phys. Rev. B* **2009**, *80* (24), 245435.
(19) West, P. R.; Ishii, S.; Naik, G. V.; Emani, N. K.; Shalaev, V. M.; Boltasseva, A. *Laser Photonics Rev.* **2010**, *4* (6), 795−808.
(20) Kim, J.; Son, H.; Cho, D. J.; Geng, B.; Regan, W.; Shi, S.; Kim, K.; Zettl, A.; Shen, Y. R.; Wang, F. *Arxiv preprint arXiv:1206.1124*, (accessed on August 1, 2012).
(21) Falkovsky, L. In *Optical properties of graphene*; IOP Publishing: London, 2008; p 012004.
(22) Li, Z.; Henriksen, E.; Jiang, Z.; Hao, Z.; Martin, M.; Kim, P.; Stormer, H.; Basov, D. N. *Nat. Phys.* **2008**, *4* (7), 532−535.

(23) Nair, R.; Blake, P.; Grigorenko, A.; Novoselov, K.; Booth, T.; Stauber, T.; Peres, N.; Geim, A. *Science* **2008**, *320* (5881), 1308−1308.
(24) Mak, K. F.; Sfeir, M. Y.; Wu, Y.; Lui, C. H.; Misewich, J. A.; Heinz, T. F. *Phys. Rev. Lett.* **2008**, *101* (19), 196405.
(25) Grosjean, T.; Mivelle, M.; Baida, F.; Burr, G.; Fischer, U. *Nano Lett.* **2011**, *11* (3), 1009−1013.
(26) Cao, H.; Yu, Q.; Jauregui, L. A.; Tian, J.; Wu, W.; Liu, Z.; Jalilian, R.; Benjamin, D. K.; Jiang, Z.; Bao, J. *Appl. Phys. Lett.* **2010**, *96*, 122106.
(27) Pinto, H.; Jones, R.; Goss, J. P.; Briddon, P. R. *Phys. Status Solidi A* **2010**, *207* (9), 2131−2136.
(28) Das, A.; Pisana, S.; Chakraborty, B.; Piscanec, S.; Saha, S.; Waghmare, U.; Novoselov, K.; Krishnamurthy, H.; Geim, A.; Ferrari, A. *Nat. Nanotechnol.* **2008**, *3* (4), 210−215.
(29) Huh, S.; Park, J.; Kim, K. S.; Hong, B. H.; Kim, S. B. *ACS Nano* **2011**, *5* (5), 3639−3644.
(30) Ni, X.; Liu, Z.; Boltasseva, A.; Kildishev, A. V. *Appl. Phys. A* **2010**, *100* (2), 365−374.
(31) Zou, Y.; Tassin, P.; Koschny, T.; Soukoulis, C. M. *Opt. Express* **2012**, *20* (11), 12198−12204.

Supplementary Online Material

Graphene is a 0.35-nm-thick monolayer of sp^2 carbon atoms. In numerical simulations, we treated graphene as an effective medium with a thickness of 1 nm. This value is reasonable considering the inhomogeneties in CVD-grown graphene, which can lead to a graphene layer that is thicker than the ideal thickness. We also performed simulations with the effective thickness as a parameter in order to verify the impact of this assumption on the final results. We found that the simulation results converged for an effective graphene thickness of 1 nm or below (see Figure S1). We also show simulations on control sample without any graphene in Fig S1. As expected and reported elsewhere, adding graphene causes the resonance to be weaker and broader (c.f. Zou Y *et al.*, Opt. Express(2012) and Kim J *et al.*, ArXiv(2012) which are references 32 and 21 in the paper).

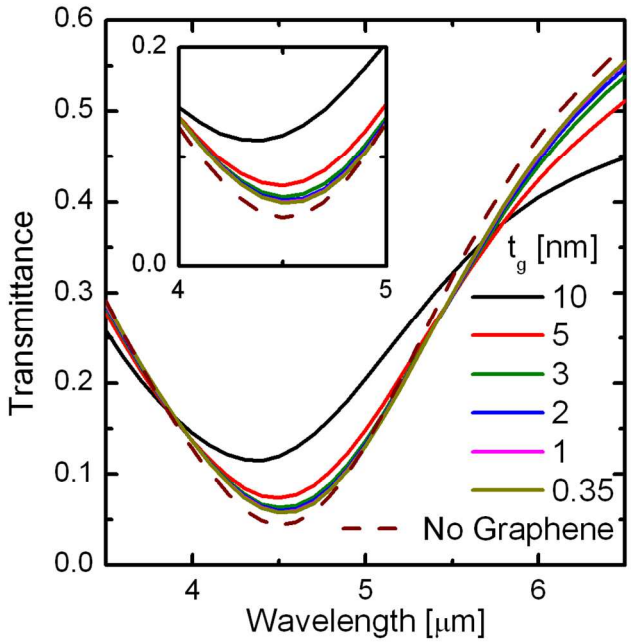

Figure S1. In numerical simulations, atomically thin graphene is assumed to have an effective thickness (t_g). The plotted simulation results show convergence for effective thickness of graphene below 1 nm. A carrier concetration of $1x10^{12}$ cm^2 and Drude scattering rate of $1x10^{-13}$s were used in calculations.

In the main text, we discussed the enhanced interaction of light with graphene in the presence of bowtie antennas. We also performed optical transmission measurements on a device without bowtie antennas. These results revealed much smaller changes in transmittance of up to only 1%, as shown in Figure S2. The incident photon is most sensitive to carrier concentration in graphene when its energy is around $2E_F$. Therefore, we see a matching peak in the normalized transmission spectrum. A gate voltage of 30V results in $2E_F$ peak at 0.5eV, which corresponds to a carrier density of $4.6x10^{12}$ cm^{-2}. At low gate voltages we expect the carrier concentration to be below $1x10^{12}$ cm^{-2}. We suspect that the peaks are not clear at low voltages because of the lower peak amplitudes and charge inhomogeneities in graphene.

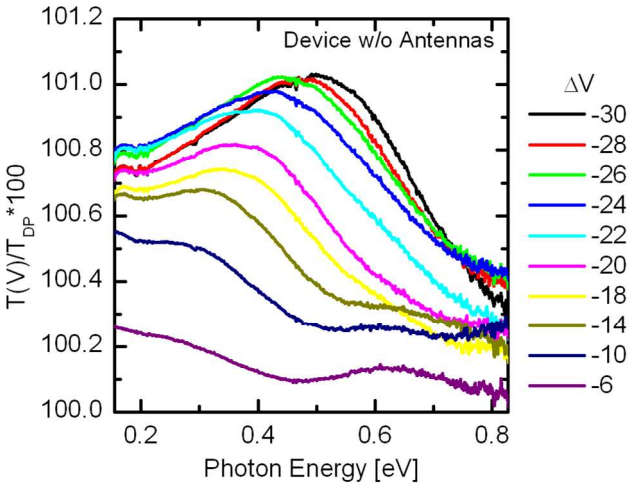

Figure S2. Optical transmission measurements for a device without bowtie antennas. The change in the observed transmittance is about 1% and is far smaller than the changes observed with bowtie antennas as shown in Figures 4 and 5 of the main text.